Table S1. Cryo-EM data collection, refinement, and validation statistics

	Csy-AcrIF4-dsDNA-overall	Csy-AcrIF4-dsDNA-Cas8f	Csy-AcrIF4-dsDNA-Cas6f
Data collection and processing			
EMDB code	EMD-33837		
PDB code	7YHS		
Electron microscopy		Titan Krios	
Camera		K3	
Magnification		29000×	
Voltage		300 kV	
Defocus range (μm)		-1.3 to -1.8	
Electron exposure (e-/Å^2)		50	
Pixel size (Å)		0.97	
Exposure rate (e$^-$/A^2/sec)		20	
Number of frames per movie		32	
Automation software		SerialEM	
Micrographs collected		839	
Data processing software		RELION 3.1	
Symmetry imposed	*C*1	*C*1	*C*1
Total extracted particles		621,597	
Total refined particles	117,510	49,498	93,188
Final particles	117,510	49,498	93,188
Map resolution (FSC=0.143/Å)	3.37	3.59	3.96
Local resolution range (Å)	2.4-4.4	2.4-4.4	3.2-5.4
Refinement			
Initial Model (PDB code)	6NE0		
Refinement Package	Phenix 1.19 (real space refinement)		
Model resolution (FSC=0.5/Å)	3.43		
Map sharpening B factor (Å^2)	-20		
Map CC	0.64		
Model composition			
Non-hydrogen atoms	24,082		
Protein residues	2949		
Nucleotides	109		
B factors (Å^2)			
Protein	28.37		
Nucleotides	55.24		
R.m.s. deviations			
Bond lengths (Å)	0.008		
Bond angles (°)	1.137		
Validation			
MolProbity score	2.54		
EMRinger score	1.68		
Clash score	7.89		
Poor rotamers (%)	7.02		
C-beta deviations	0		
CaBLAM outliers	5.41		
Ramachandran plot (%)			
Favored	92.42		
Allowed	7.55		

Outlier	0.03

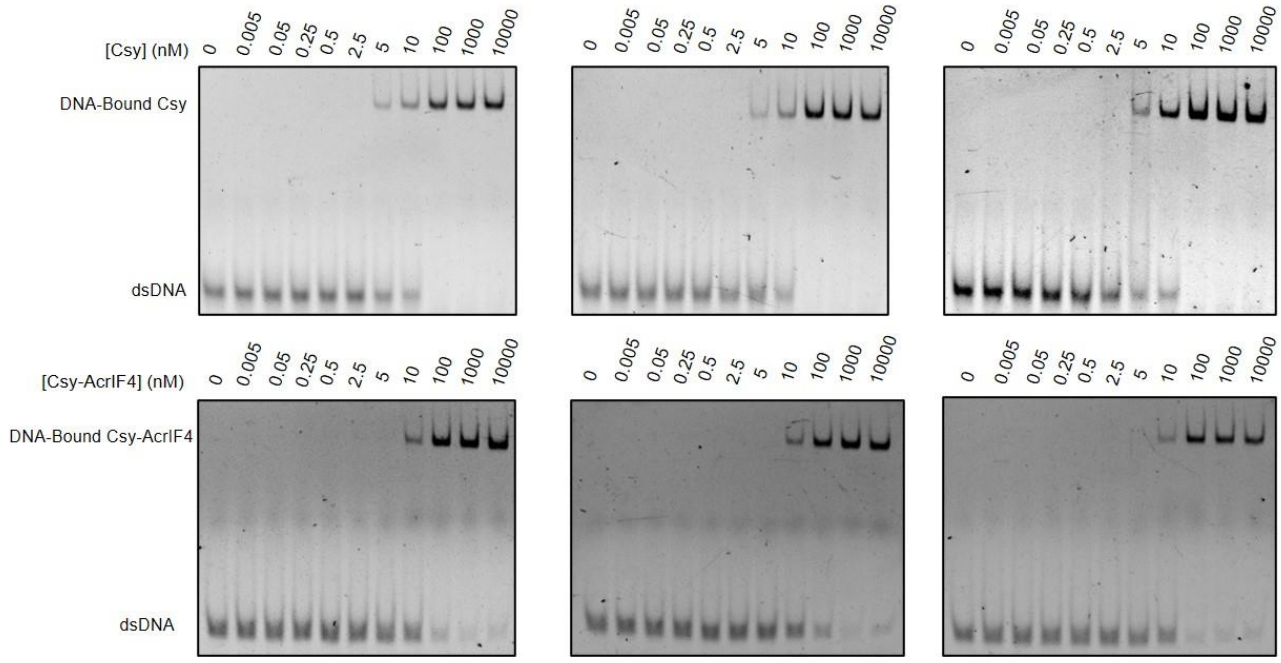

Figure S1 Binding between dsDNA and the AcrIF4-bound or apo Csy complex

DNA binding assays were performed by incubating a concentration gradient (0, 0.005, 0.05, 0.25, 0.5, 2.5, 5, 10, 100, 1000, 10000 nM) of the Csy (or Csy-AcrIF4) complex with 16 nM of 54 bp dsDNA (5′-FAM in the TS).

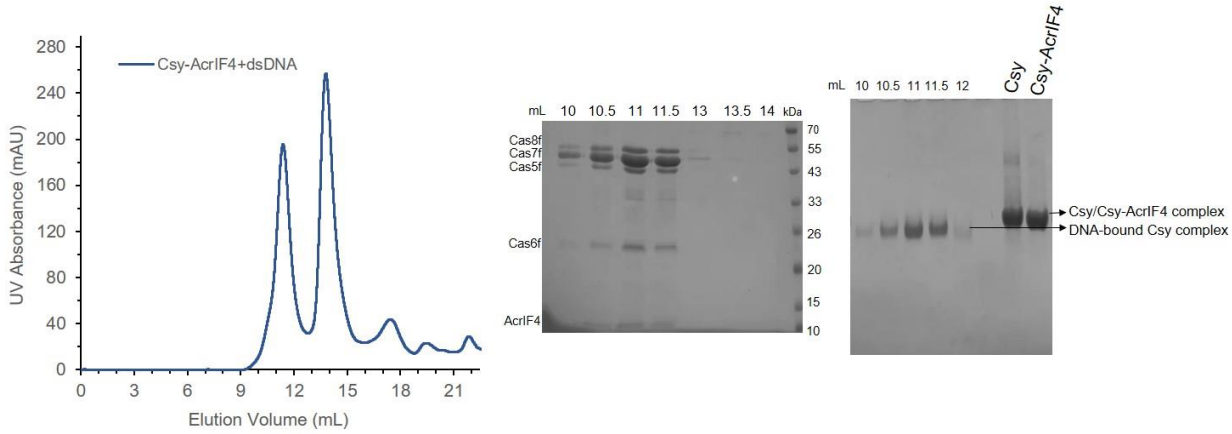

Figure S2 dsDNA co-elutes with the Csy-AcrIF4 complex

Gel filtration profiles of the mix of Csy-AcrIF4/dsDNA. The UV absorbance at 280 nm is shown. The SDS-PAGE and native PAGE of the peak fractions are shown on the right.

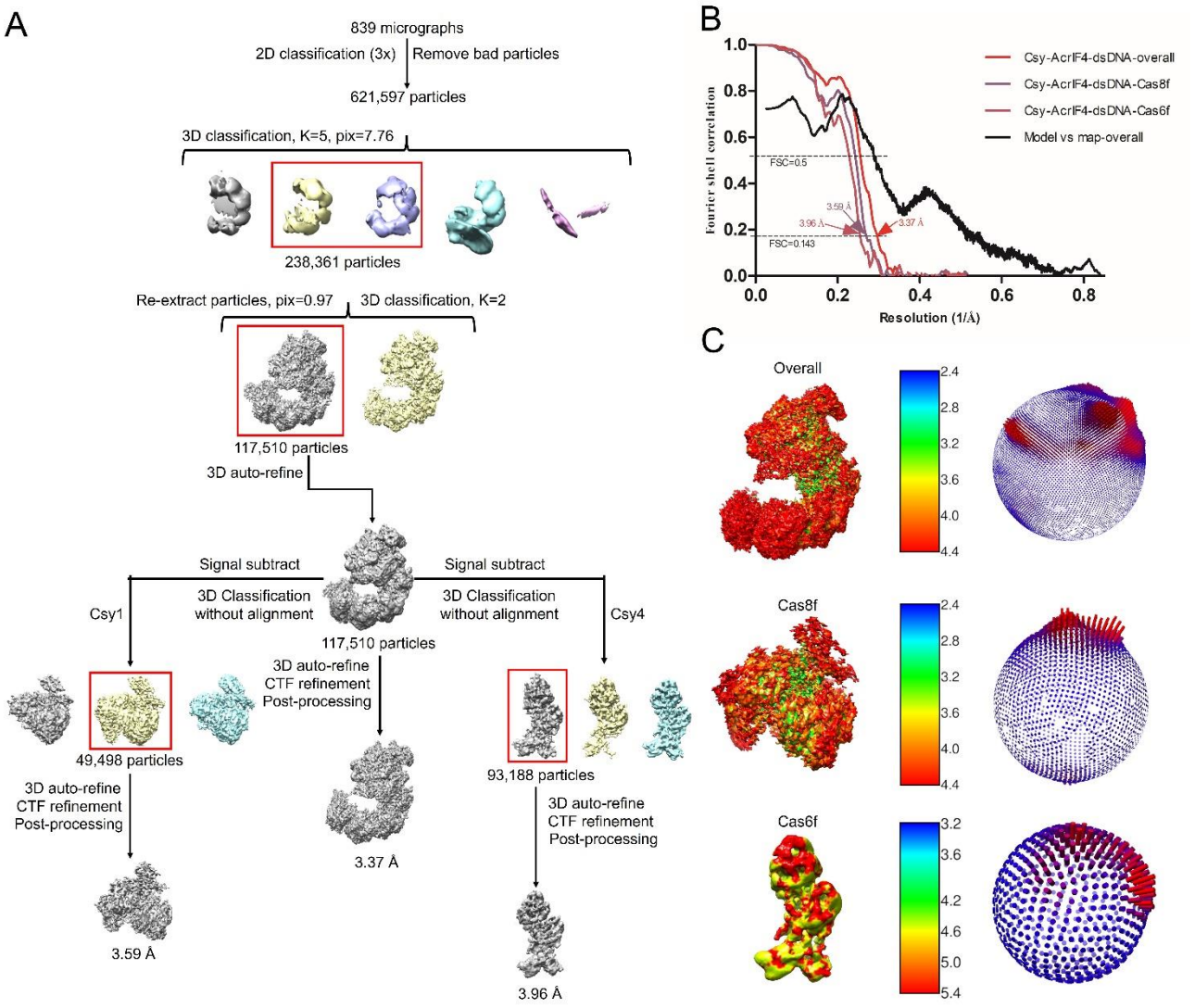

Figure S3 Cryo-EM image processing for the Csy-AcrIF4-dsDNA complex

(A) Representative data processing of Csy-AcrIF4-dsDNA complex. 3D classification, signal subtraction, 3D-auto refinement, CTF Refinement and post-processing were performed with subregion of Cas8f and Cas6f in RELION 3.1.

(B) Representative the gold-standard Fourier Shell Correlation (FSC=0.143) curves and model vs map curve (FSC=0.5) of Csy-AcrIF4-dsDNA complex, Cas8f and Cas6f.

(C) Local resolution estimation and particle orientation distributions of the Csy-AcrIF4-dsDNA complex, Cas8f and Cas6f.

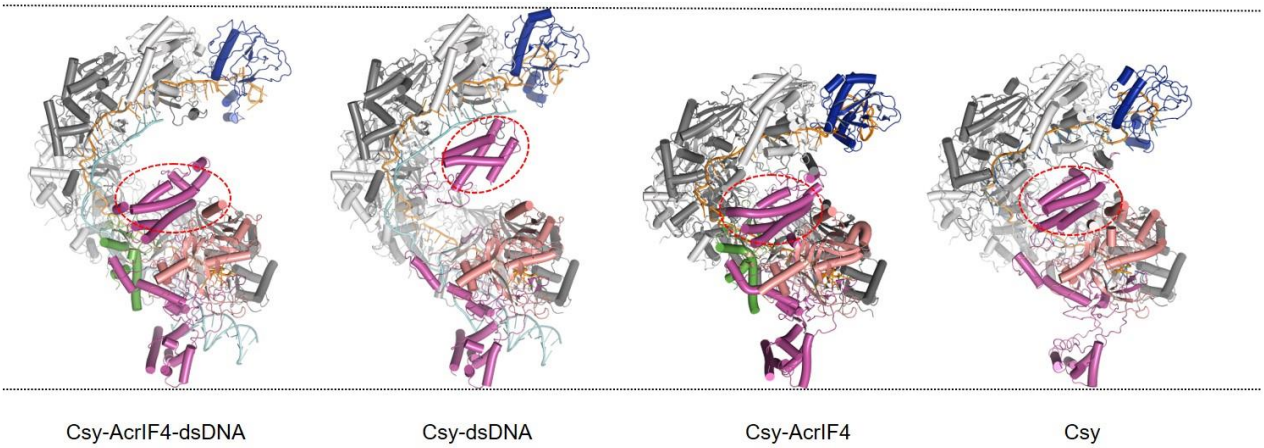

Figure S4 Side-by-side comparison of the Csy-AcrIF4-dsDNA, Csy-dsDNA, Csy-AcrIF4 and Csy structures

Side-by-side comparison of the Csy-AcrIF4-dsDNA (this study), Csy-dsDNA (PDB code: 6NE0), Csy-AcrIF4 (PDB code: 7JZW) and Csy (PDB code: 6B45) structures. The Cas8f HB is marked in a circle.

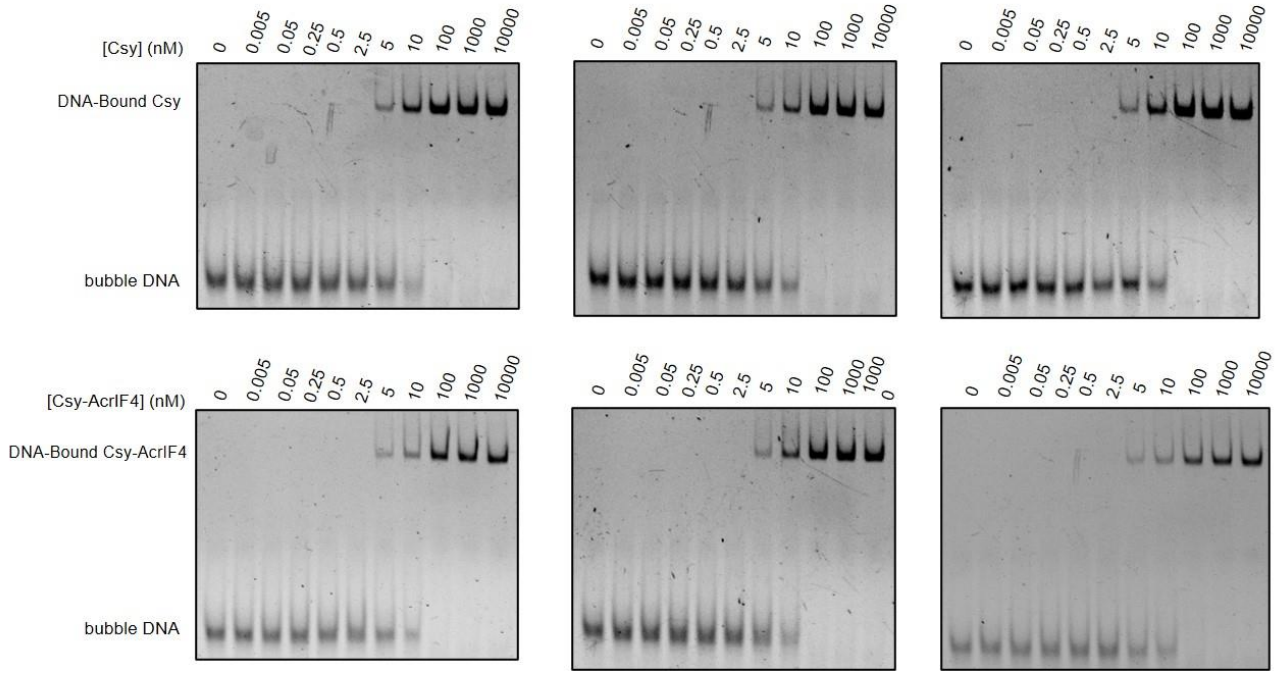

Figure S5 Binding between bubble dsDNA and the AcrIF4-bound or apo Csy complex
DNA binding assays were performed by incubating a concentration gradient (0, 0.005, 0.05, 0.25, 0.5, 2.5, 5, 10, 100, 1000, 10000 nM) of the Csy (or Csy-AcrIF4) complex with 16 nM of 54 bp dsDNA bubble (5′-FAM in the TS).

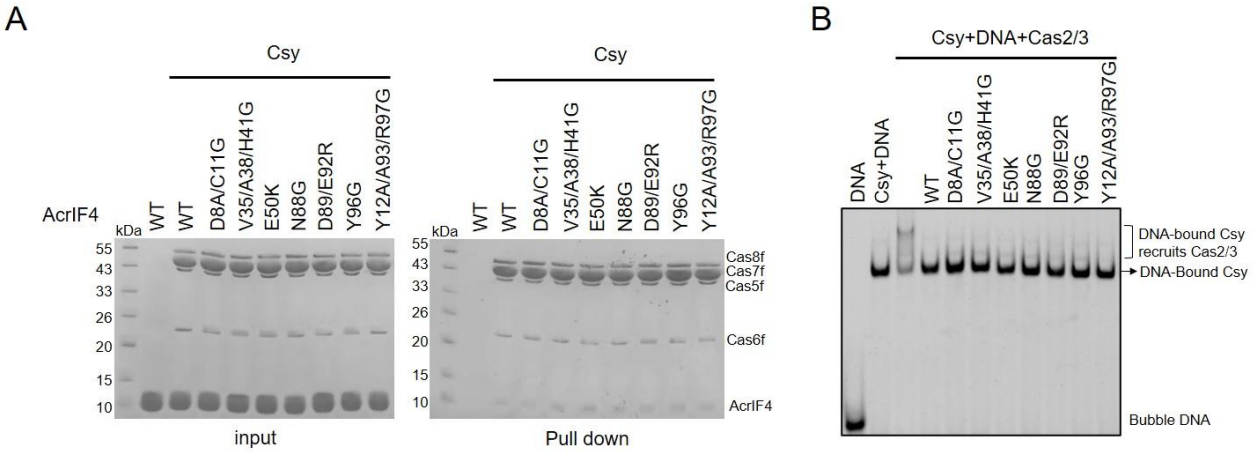

Figure S6 AcrIF4 mutations on a specific interface do not result in marked Csy binding defect

(A) Reactions were performed with 6 μM Csy complex and 180 μM AcrIF4 or its mutants for 30 min at 37℃, and then the mixtures were incubated with Ni-NTA beads for 30 min at 4℃. Samples of input and pull-down were separated using SDS-PAGE after washing three times.

(B) Mutations of the interface residues of AcrIF4 did not affect its inhibition capacity of Cas2/3 recruitment. Reactions were performed with 1.6 μM Csy complex, 0.1 μM 54-bp bubble dsDNA (5′-FAM in the target DNA strand), 3.2 μM AcrIF4, and 0.8 μM Cas2/3. Reactions were independently repeated three times with similar results.